

### Supporting Information for

The impact of chalcogen-substitution element and initial spectroscopic state on excited-state relaxation pathways in nucleobase photosensitizers: a combination of static and dynamic studies

Min Xie,<sup>a</sup> Shuang-xiao Ren,<sup>a</sup> Die Hu,<sup>a</sup> Ji-meng Zhong,<sup>a</sup> Jie Luo,<sup>a</sup> Yin Tan,<sup>a</sup> Yan-ping Li,<sup>b</sup> Li-ping Si,<sup>a</sup> Jun Cao,<sup>\*,a,c</sup>

<sup>a</sup>*School of Materials Science and Hydrogen Energy & Guangdong Key Laboratory for Hydrogen Energy Technologies, Foshan University, Foshan, Guangdong, 528000, P. R. China*

<sup>b</sup>*School of Medicine, Foshan University, Foshan, Guangdong, 528000, P. R. China*

<sup>c</sup>*Guizhou Provincial Key Laboratory of Computational Nano-Material Science, Guizhou Education University, Guiyang, Guizhou, 550018, P. R. China*

#### Contents:

1. **Table S1.** Relative energies (eV) of different states at the MS-CASPT2(12,10)/ ANO-RCC-VDZP optimized minima and crossing points.
2. **Table S2.** Spin-orbit couplings between  $S_2$  and  $T_2$  at the  $S_2/S_1$  points and between  $S_1$  and  $T_2$  at the  $S_1$  minima of both molecules.
3. **Figure S1.** Molecular orbitals included in the active space for each molecule.
4. **Figure S2.** The MS-CASPT2(12,10)/ANO-RCC-VDZP optimized minimum and crossing structures.
5. **Figure S3.** LIICs computed at the LR-TD- $\omega$ B97XD/6-31G\* level of theory based on the MS-CASPT2(12,10)/ANO-RCC-VDZP optimized critical points.
6. **Figure S4.** Time evolution of some chosen geometrical parameters from dynamics of the  $S_2$  state of 6TG.
7. **Figure S5.** Time evolution of some chosen geometrical parameters from dynamics of the  $S_2$  state of 6SG.
8. **Figure S6.** Additional calculations of the energy gaps and spin-orbit coupling magnitudes at the  $S_2/S_1$ ,  $S_2/T_2$ , and  $S_2/T_3$  crossing points of 6SG, and the energy gaps and spin-orbit coupling magnitudes between  $S_2$  and  $T_2$  and between  $S_2$  and  $T_3$  at the  $S_2/S_1$  hopping points of 6TG.
9. **Figure S7.** Distribution of crossing time, spin-orbit coupling vs energy gap, and geometrical parameters for the  $S_1 \rightarrow$  triplet crossings from dynamics of the  $S_2$  state of 6SG.
10. **Figure S8.** Time evolution of some chosen geometrical parameters from dynamics of the  $S_3$  state of 6TG.
11. **Figure S9.** Geometrical parameters of hopping points involved in the  $S_3 \rightarrow S_2 \rightarrow S_1$  internal conversion for 6TG.
12. **Figure S10.** Time evolution of some chosen geometrical parameters from dynamics of the  $S_3$  state of 6SG.
13. **Figure S11.** Geometrical parameters of hopping points involved in the  $S_3 \rightarrow S_2 \rightarrow S_1$  internal conversion for 6SG.
14. **Figure S12.** Spin-orbit coupling vs energy gap for those between  $S_2$  and  $T_2$  and between  $S_2$  and  $T_3$  at the  $S_2 \rightarrow S_1$  and  $S_2 \rightarrow T_{2,3}$  crossing points from dynamics of the  $S_3$  state of both molecules.
15. **Figure S13.** Distribution of crossing time, spin-orbit coupling vs energy gap, and geometrical parameters for the  $S_1 \rightarrow$  triplet crossings from dynamics of the  $S_3$  state of both molecules.

**Table S1.** Relative energies (eV) of different states at the optimized minima and crossing points in different level of theory. The LR-TD- $\omega$ B97XD/6-31G\* calculated energies are based on MS-CASPT2 optimized geometries and given in italic. The oscillator strengths are given in parentheses.

Energy Geometry		6TG		6SG	
		Based on MS-CASPT2(12,10)/ ANO-RCC-VDZP ptimized structures	MS-CASPT2//CASSCF (14,12)/ANO-L optimized structures (from Ref.45 in main text)	Based on MS-CASPT2(12,10)/ANO-RCC-VDZP optimized structures	MS-CASPT2//CASSCF(12,10)/cc-pVDZ optimized structures (from Ref.51 in main text)
S <sub>0</sub> minimum	S <sub>0</sub>	0.0 <i>0.0</i>	0.0	0.0 <i>0.0</i>	0.0
	S <sub>1</sub>	3.41 3.38	3.36	2.93 2.94	2.61
	S <sub>2</sub>	4.0(0.50) <i>4.33</i>	4.05(0.54)	3.59(0.52) <i>4.0</i>	3.39(0.24)
	S <sub>3</sub>	4.85 (0.11) <i>4.98</i>	4.90(0.144)	4.53 (0.05) <i>4.75</i>	
	T <sub>1</sub>	3.03 2.63	3.10	2.68 2.21	2.40
	T <sub>2</sub>	3.37 3.08	3.31	2.92 2.65	2.56
	T <sub>3</sub>	4.20 3.79	4.24	4.07 3.75	
S <sub>1</sub> minimum	S <sub>1</sub> /T <sub>2</sub> /T <sub>1</sub>	3.13/3.09/2.89 <i>3.23/2.89/2.49</i>	3.18	2.69/2.66/2.50 <i>2.93/2.59/2.09</i>	2.46
S <sub>2</sub> minimum	S <sub>2</sub>	3.71 <i>4.23</i>	3.78	3.26 <i>3.89</i>	3.04
T <sub>1</sub> minimum	T <sub>1</sub>	2.76 <i>2.44</i>	3.00	2.44 <i>2.03</i>	2.24
S <sub>2</sub> /S <sub>1</sub>	S <sub>2</sub> /S <sub>1</sub> /T <sub>2</sub>	4.04/4.04/4.02 <i>4.42/4.15/3.93</i>	3.96	3.68/3.66/3.68 <i>4.28/3.94/3.74</i>	
T <sub>1</sub> /S <sub>0</sub>	T <sub>1</sub> /S <sub>0</sub>	3.06/3.06 <i>3.07/3.48</i>	3.16	2.73/2.73 <i>2.70/3.23</i>	2.35/2.22
S <sub>1</sub> ( $\pi_{45}\pi_{23}^*$ )/S <sub>0</sub>	S <sub>1</sub> /S <sub>0</sub>	4.73/4.71 <i>5.44/5.07</i>	3.90	4.28/4.27 <i>5.03/4.69</i>	
S <sub>1</sub> ( $n_{10}\pi_{610}^*$ )/S <sub>0</sub>	S <sub>1</sub> /S <sub>0</sub>	4.05/4.03	4.87	3.69/3.68	

**Table S2.** Spin-orbit coupling (SOC) magnitudes (cm<sup>-1</sup>) between S<sub>2</sub> and T<sub>2</sub> at the S<sub>2</sub>/S<sub>1</sub> points and between S<sub>1</sub> and T<sub>2</sub> at the S<sub>1</sub> minima of both molecules, calculated in different level of theory.

SOCs Region		6TG		6SG	
		MS-CASPT2	LR-TDDFT	MS-CASPT2	LR-TDDFT
S <sub>2</sub> /S <sub>1</sub>		78.5	63.0	387.1	412.0
S <sub>1</sub> minimum		88.6	85.1	427.3	401.3

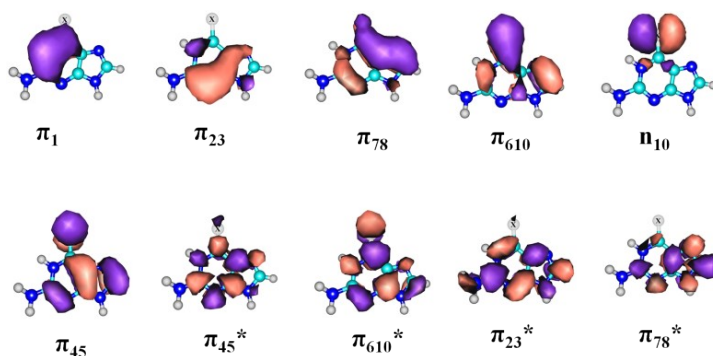


**Figure S1.** Molecular orbitals included in the active space. X=S or Se.

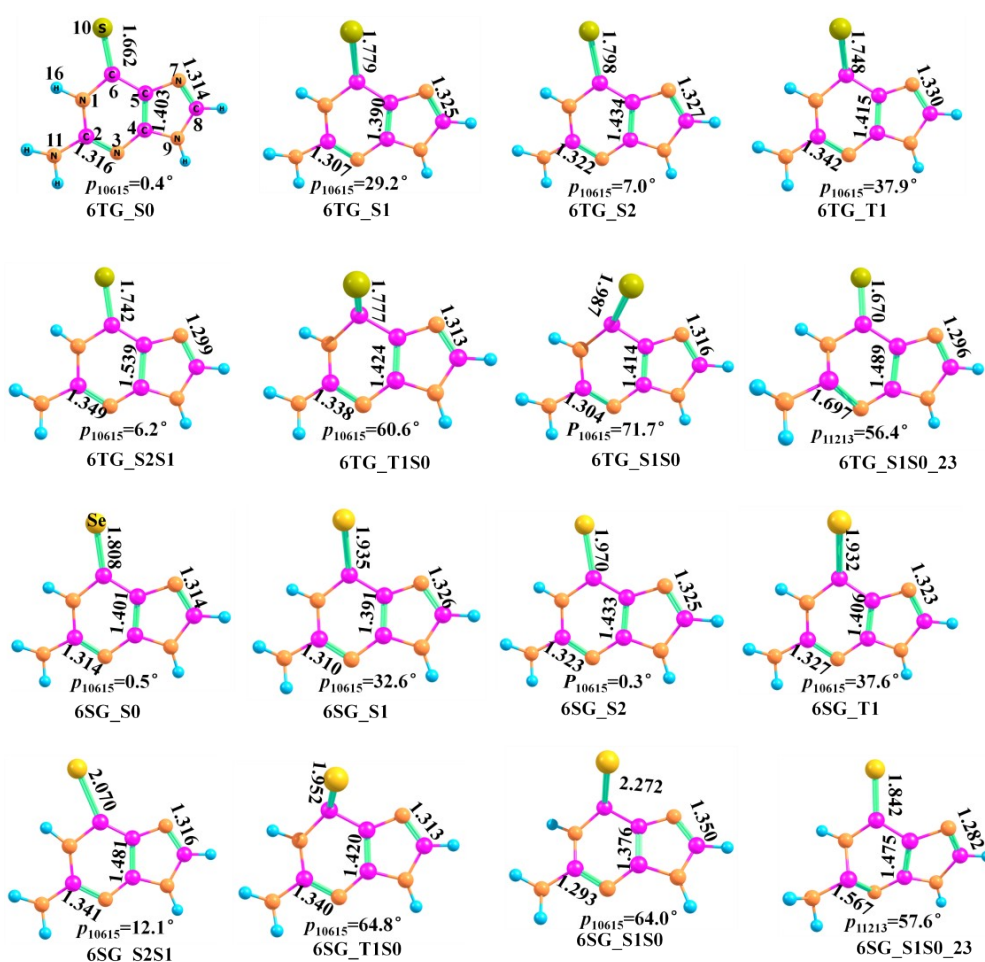


**Figure S2.** The MS-CASPT2(12,10)/ANO-RCC-VDZP optimized minimum and crossing structures, along with chosen geometrical parameters (bond-length in Å, and angle in °). The atom labels are given in the  $S_0$  minimum of 6TG (6TG\_S0). Minima in the  $S_1(n_s\pi^*)$ ,  $S_2(\pi\pi^*)$ ,  $T_1(\pi\pi^*)$  states of 6TG are referred as 6TG\_S1, 6TG\_S2, and 6TG\_T1, respectively, and crossing points between  $S_2(\pi\pi^*)$  and  $S_1(n_s\pi^*)$ , between  $T_1(\pi\pi^*)$  and  $S_0$ , between  $S_1(n_s\pi^*)$  and  $S_0$ , and between  $S_1(\pi\pi_{23}^*)$  and  $S_0$  are referred as 6TG\_S2S1, 6TG\_T1S0, 6TG\_S1S0, and 6TG\_S1S0\_23, respectively. For 6SG, minima in the  $S_0$ ,  $S_1(n_s\pi^*)$ ,  $S_2(\pi_s\pi^*)$ ,  $T_1(\pi\pi^*)$  states are referred as 6SG\_S0, 6SG\_S1, 6SG\_S2, and 6SG\_T1, respectively, and crossing points between  $S_2(\pi\pi^*)$  and  $S_1(n_s\pi^*)$ , between  $T_1(\pi\pi^*)$  and  $S_0$ , between  $S_1(n_s\pi^*)$  and  $S_0$ , and between  $S_1(\pi\pi_{23}^*)$

and  $S_0$  are referred as 6SG\_S2S1, 6SG\_T1S0, 6SG\_S1S0, and 6SG\_S1S0\_23, respectively.

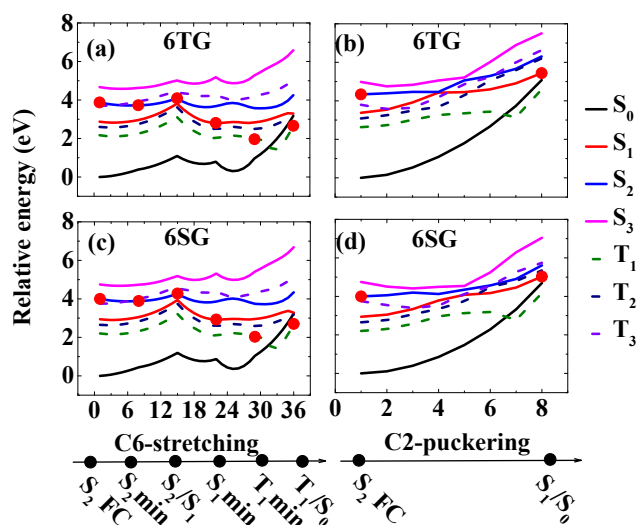


**Figure S3.** LIICs computed at the LR-TD- $\omega$ B97XD/6-31G\* level of theory based on the MS-CASPT2(12,10)/ANO-RCC-VDZP optimized structures.

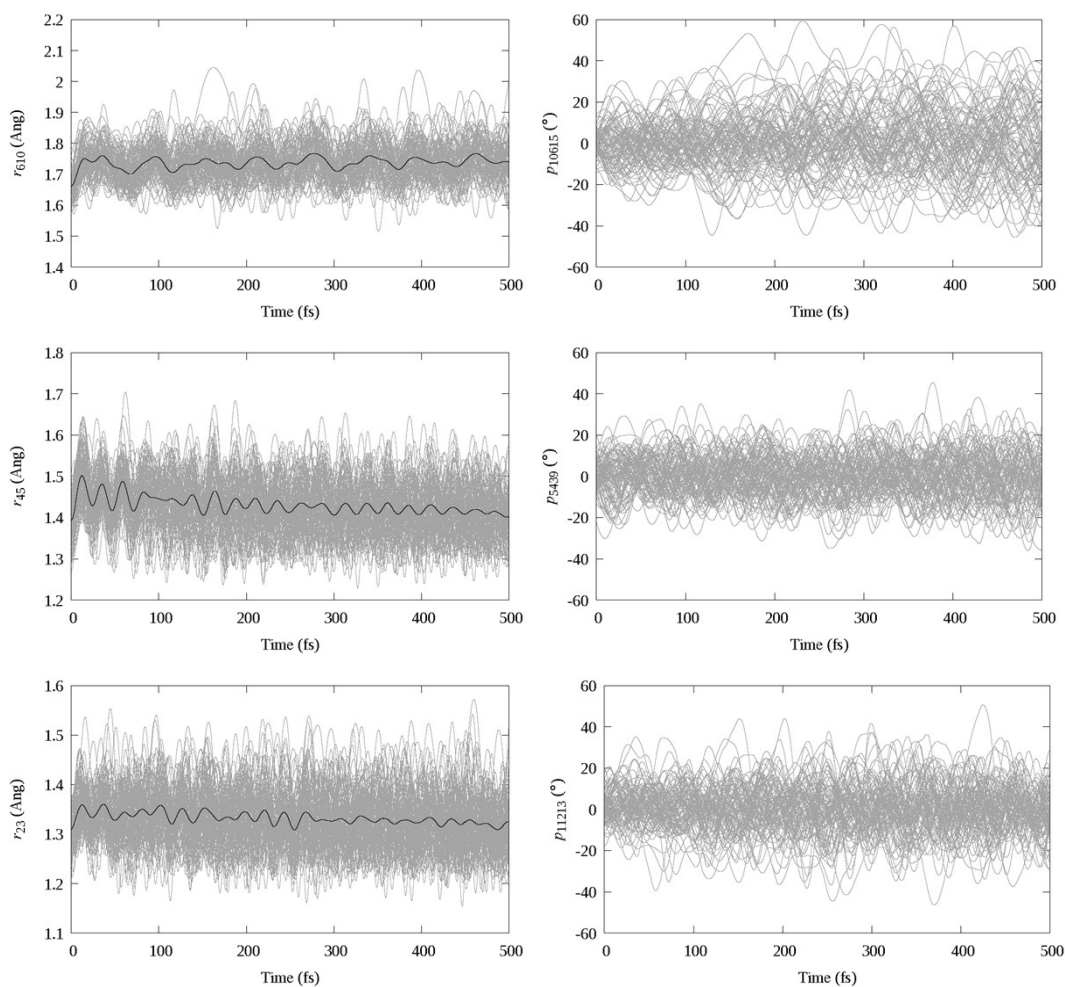


**Figure S4.** Time evolution of some chosen geometrical parameters from dynamics of the  $S_2$  state of 6TG.

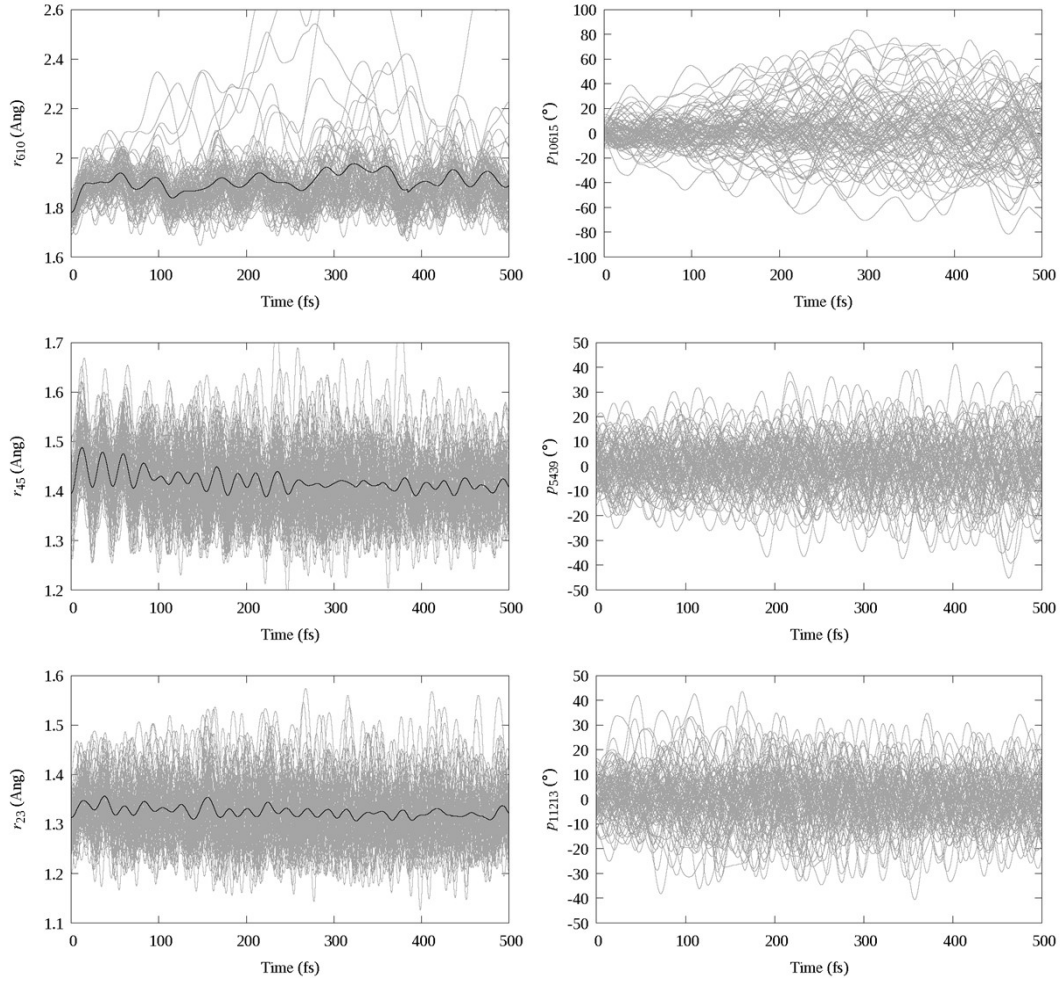


**Figure S5.** Time evolution of some chosen geometrical parameters from dynamics of the  $S_2$  state of 6SG.

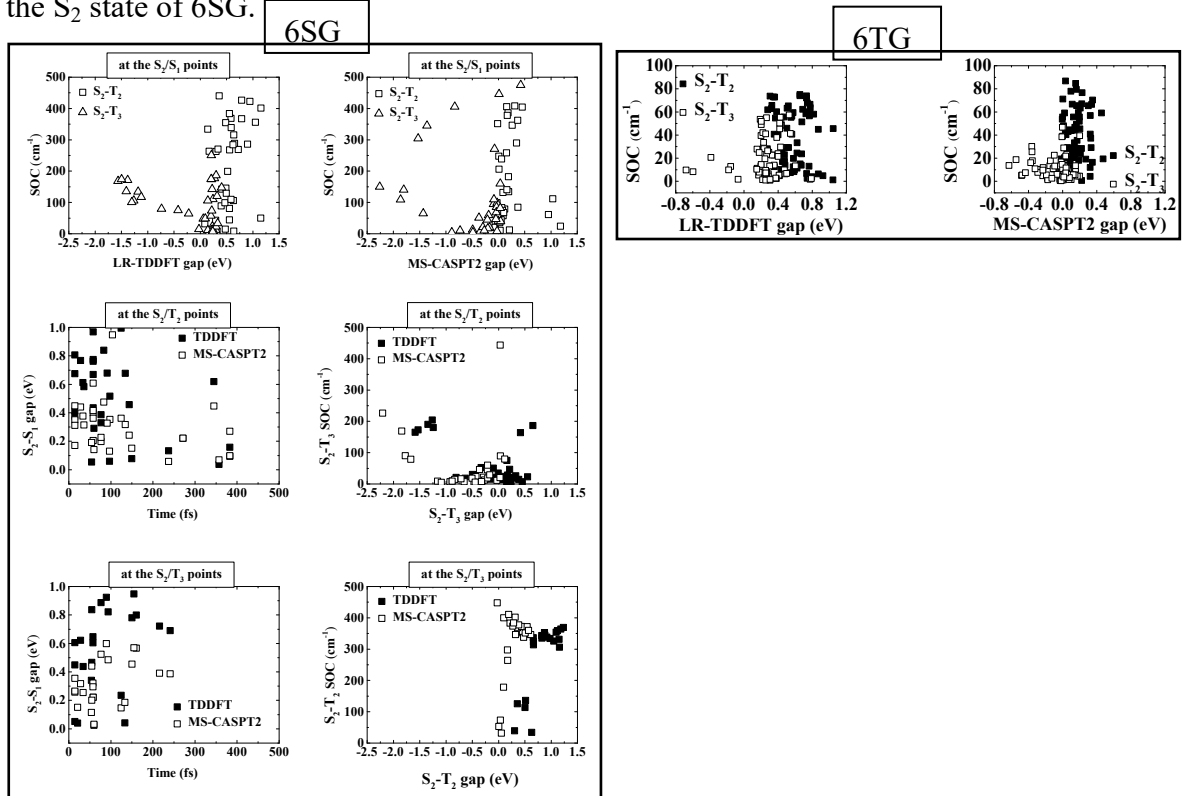


**Figure S6.** Additional calculations of the energy gaps and spin-orbit coupling (SOC) magnitudes at the  $S_2/S_1$ ,  $S_2/T_2$ , and  $S_2/T_3$  crossing points of 6SG, and the energy gaps and spin-orbit coupling magnitudes between  $S_2$  and  $T_2$  and between  $S_2$  and  $T_3$  at the  $S_2/S_1$  hopping points of 6TG.

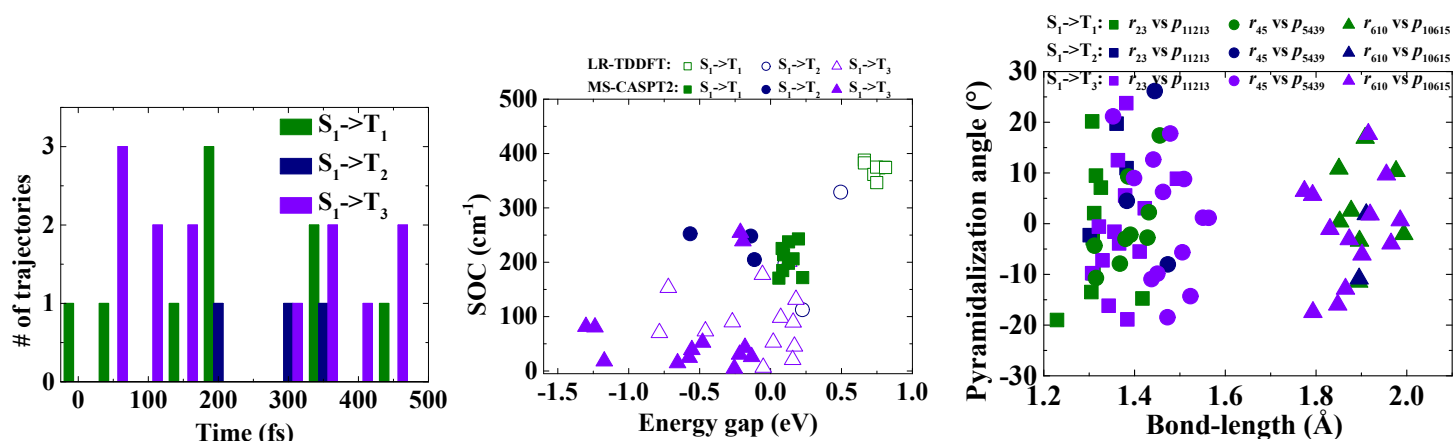


**Figure S7.** Distribution of crossing time, spin-orbit coupling (SOC) vs energy gap, and geometrical parameters for the  $S_1 \rightarrow$  triplet crossings from dynamics of the  $S_2$  state of 6SG.

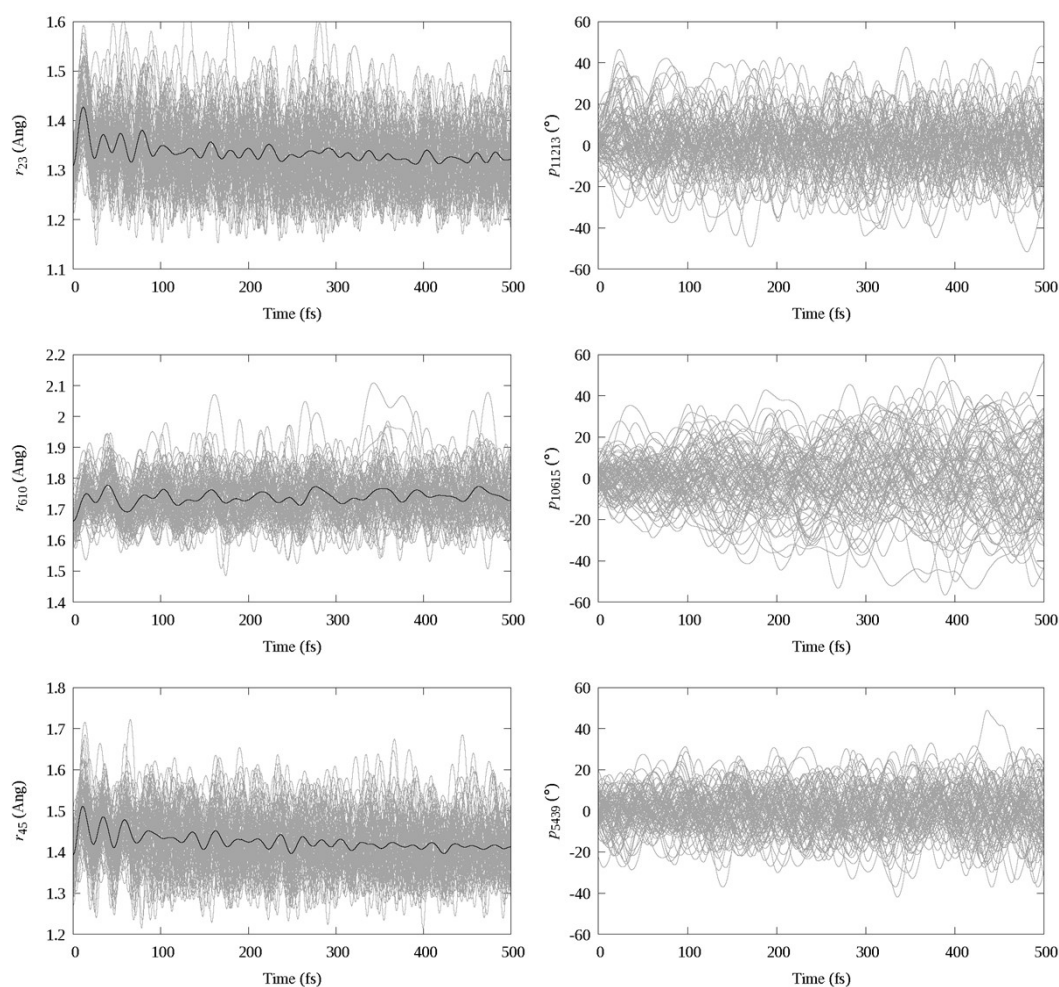


**Figure S8.** Time evolution of some chosen geometrical parameters from dynamics of

the  $S_3$  state of 6TG.

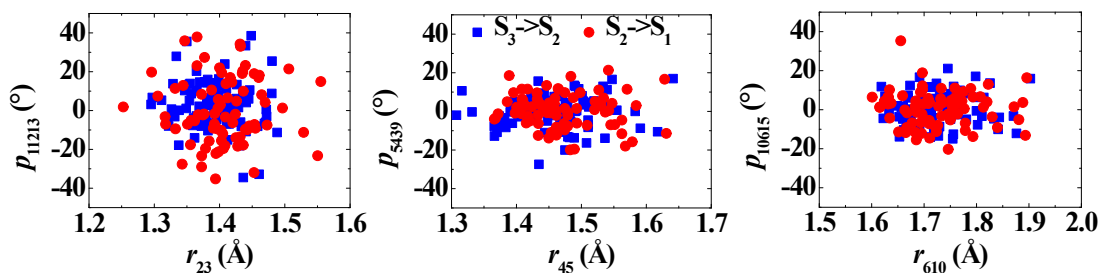


**Figure S9.** Geometrical parameters of hopping points involved in the  $S_3 \rightarrow S_2 \rightarrow S_1$  internal conversion for 6TG.

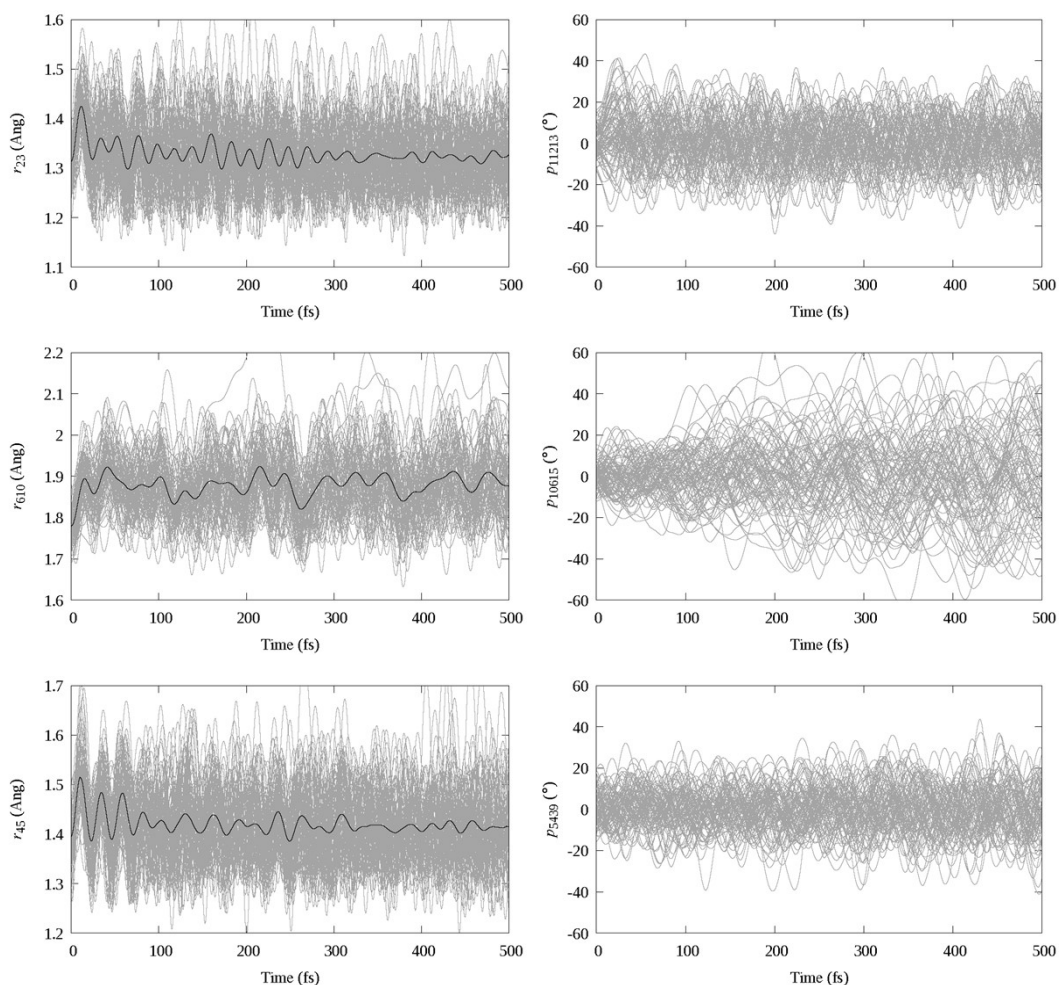


**Figure S10.** Time evolution of some chosen geometrical parameters from dynamics of the  $S_3$  state of 6SG.

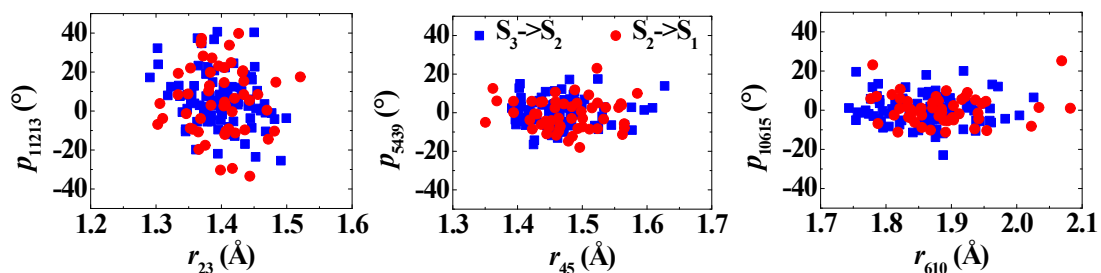


**Figure S11.** Geometrical parameters of hopping points involved in the  $S_3 \rightarrow S_2 \rightarrow S_1$

internal conversion for 6SG.

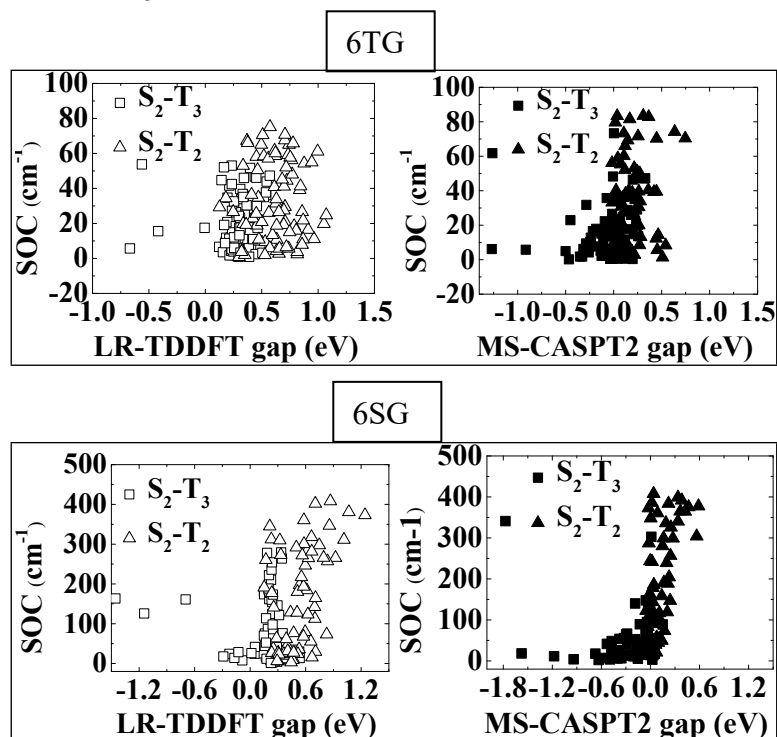


**Figure S12.** Spin-orbit coupling (SOC) vs energy gap for those between  $S_2$  and  $T_2$  and between  $S_2$  and  $T_3$  at the  $S_2 \rightarrow S_1$  and  $S_2 \rightarrow T_{2,3}$  crossing points from dynamics of the  $S_3$  state of both molecules, calculated in different level of theory.

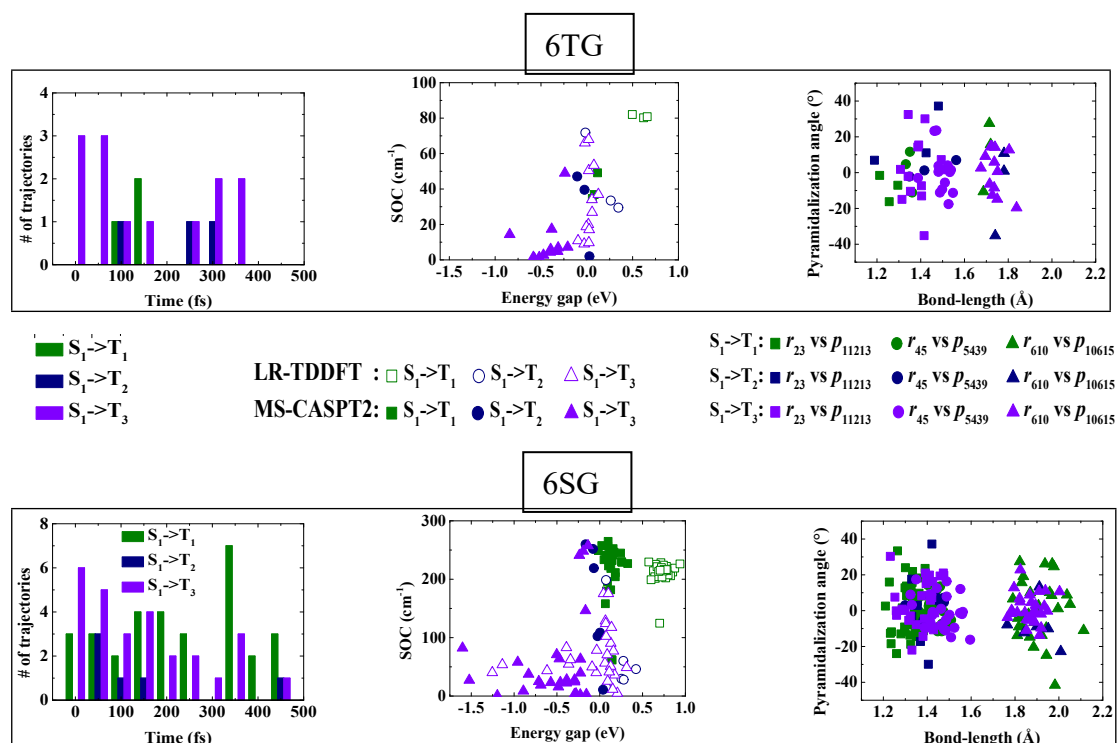


**Figure S13.** Distribution of crossing time, spin-orbit coupling (SOC) vs energy gap, and geometrical parameters for the  $S_1 \rightarrow$  triplet crossings from dynamics of the  $S_3$  state of both molecules.